Air Quality, Atmosphere & Health (2024) 17:1253–1264
https://doi.org/10.1007/s11869-022-01198-9

Modelling the influence of road elevation on pollutant dispersion

James O'Neill[1] · Martin Seaton[1] · Kate Johnson[1] · Jenny Stocker[1] · Rohan Patel[1] · Martine Van Poppel[2] · David Carruthers[1]

Received: 30 December 2021 / Accepted: 1 April 2022 / Published online: 21 April 2022

Abstract
Local urban air quality models must be able to account for complex road geometries if they are to predict near-road concentrations accurately. This includes flyovers, which are often used to improve flow at busy junctions or to take traffic through urban greenspace. We present a new methodology for modelling elevated roads in which the plume is only allowed to grow downwards once it has left the downwind road edge, thus accounting for road shielding. This new approach has been implemented in the operational dispersion model ADMS-Urban. The updated model is validated against monitoring data from two sites located next to busy flyovers—one in London, UK, the other in Antwerp, Belgium. It is shown to perform very well compared with simulations in which the flyovers are modelled at ground level, and slightly better than simulations when the traditional approach to modelling elevated roads (no road shielding) is used. Near-ground concentrations are significantly reduced with road elevation due to (i) increased vertical source-receptor distance, (ii) greater dispersion from the source where wind speeds are higher, and (iii) reduced impact of ground-level plume reflections. Pollutant trapping in street canyons is also minimised in cases where a flyover is elevated above the local building level. A sensitivity analysis is also presented in which multiple road elevations are tested; these results can be used by urban planners when designing new flyovers or by modellers in deciding whether it is important to account for road elevation near sensitive receptors.

Keywords Elevated roads · Flyovers · Urban dispersion modelling · ADMS · Air pollution · Validation

Introduction

Urban populations are often exposed to dangerous levels of pollutants that include nitrogen oxides (NO_X) and particulate matter, which are known to adversely affect human health (Kampa and Castanas 2008). The World Health Organization recently lowered their air quality guideline levels for these (and other) pollutants, stating that significant health risks are carried with exposure to lower concentrations than previously thought (WHO 2021).

Road traffic emissions typically form the largest contributor to poor air quality in urban areas (Fenger 1999). Urban morphology has a strong influence on street-level concentrations from road traffic. For example, street canyons formed by flanking buildings can trap emissions within recirculating vortices, leading to higher concentrations than near equivalent 'open' roads (Oke 1988; Caton et al. 2003). Other complex road geometries such as flyovers and underpasses are commonly used to improve traffic flow at junctions (Sala 2013). The effects of these features on street-level concentrations are less well understood; however, source elevation has long been recognised as an effective pollutant mitigation strategy for industrial point sources (Kumar et al. 2015).

Local urban air quality models must be able to account for these road geometry effects to aid accurate prediction. Good progress has been made in recent years on modelling street canyon effects (Vardoulakis et al. 2007; Hood et al. 2021). Conversely, even state-of-the-art operational models such as ADMS-Urban (Carruthers et al. 2000) and AERMOD (Cimorelli et al. 2005; Snyder et al. 2013) still use a relatively simplified approach to modelling flyovers; the road source height is simply raised without taking into account the shielding effect of the road surface on downward dispersion. While computational fluid dynamic (CFD) simulations are able to explicitly resolve plume interactions with individual obstacles such as flyovers

✉ James O'Neill
james.oneill@cerc.co.uk

[1] Cambridge Environmental Research Consultants, Cambridge, UK

[2] VITO, Mol, Belgium

(Tominaga and Stathopoulos 2013), their large computational cost still makes them unfeasible for operational purposes. Therefore, there exists a need for improved elevated road parameterisations within operational urban dispersion models. One such approach is presented in this paper.

Ideally, urban dispersion models should be validated against high-quality field data. While numerous measurement campaigns have been conducted near-ground-level roads (e.g. Hitchins et al. 2000; Beckerman et al. 2008; Baldwin et al. 2015), relatively few are performed near elevated roads. Joerger and Pryor (2018) sampled particulate number concentrations either side of an elevated freeway in Syracuse, NY State. They found that concentrations were lower than those from similar studies of ground-level highways but observed a slower rate of decay with distance from the road, indicating a wider area of impact. Lu et al. (2020) and Wu et al. (2022) both analysed measurements collected near elevated roads within street canyons in central Shanghai. The former used sensors on the exterior of an adjacent building at multiple floor levels to infer vertical concentration patterns and observed a bimodal distribution with a larger ground-level peak from the street-level road and a second, less pronounced, peak from the elevated road. The latter concluded that the flyover structure can inhibit upward diffusion from the street-level road, increasing concentrations below it. Van Poppel et al. (2012) collected measurements near a more open motorway flyover in Antwerp, Belgium, comparing them to measurements taken next to an adjacent ground-level section of the motorway in order to quantify the effect of raising the road height. Data from continuous air quality reference monitors, such as from the UK Automatic Urban and Rural Network (AURN; Defra 2021), located in the vicinity of elevated road sections are also suitable for evaluating urban dispersion models that account for road elevation.

Reduced-scale wind-tunnel and/or high-fidelity CFD simulated datasets are also commonly used for validation purposes. Heist et al. (2009) tested various road configurations in a wind tunnel, including cuttings and embankments, but not flyovers where the wind can pass underneath the elevated road carriageway. A number of studies have utilised CFD models to investigate the situation in which an elevated road is located within a deep street canyon that extends above the elevated road height (e.g. Hang et al. 2017; Cai et al. 2020; Zhi et al. 2020). Hang et al. (2017) found that elevating the road reduces ground-level exposure within the street canyon, while Zhi et al. (2020) showed that the flyover structure can significantly affect the flow structure within the canyon. While such studies are useful, these types of urban configuration are more commonly found in large Asian cities than in UK/European cities where aspect ratios are typically comparatively small.

This paper is structured as follows. The "New modelling approach" section presents a new methodology for modelling elevated roads in a Gaussian-type dispersion model. The "Evaluation approach" section describes the model evaluation approach, including details of two monitoring sites (London, UK, and Antwerp, Belgium) as well as model setup information. The "Results and discussion" section presents model results and provides discussion. Finally, conclusions are drawn in the "Conclusions" section.

Methodology

New modelling approach

A new approach to modelling elevated roads has been implemented in ADMS-Urban / ADMS-Roads version 5.0.1 (hereafter referred to as 'ADMS'). As with the traditional approach, the finite-width road is first decomposed into a number of 1–D crosswind elements, each of which takes a source strength Q ($\mathrm{gm^{-1}s^{-1}}$) that is proportional to the local spacing between elements and such that their sum is equal to the overall emission rate of the road (CERC 2021). The concentration is then taken as the sum of the individual contributions from each element, calculated using the following expression:

$$C = \frac{Q}{U} g(y) f(z), \tag{1}$$

where U is the wind speed ($\mathrm{ms^{-1}}$), and $g(y)$ and $f(z)$ are the crosswind and vertical concentration distribution functions, respectively, each of which must integrate to unity.

With the traditional approach, the vertical concentration distribution is taken as a single Gaussian function (or skewed Gaussian in convective conditions) with reflections at the ground:

$$f(z) = \frac{1}{\sqrt{2\pi}\sigma_z} \left\{ exp\left(\frac{-(z - z_p)^2}{2\sigma_z^2} \right) + exp\left(\frac{-(z + z_p)^2}{2\sigma_z^2} \right) \right\}. \tag{2}$$

Here, σ_z is the vertical plume spread which takes an initial value of $h_0 = 1\mathrm{m}$ before growing with downwind distance, and z_p is the plume centreline height (m) which is taken as h_0 above the road surface. There are also reflections at the top of the boundary layer in the presence of a temperature inversion, but these reflection terms have been omitted here for brevity. While this traditional approach is appropriate for elements at the downwind edge of the road, there is nothing to account for the shielding effects of the elevated road surface for elements nearer the upwind edge of the road; material is allowed to disperse freely through the road surface (Fig. 1(a)).

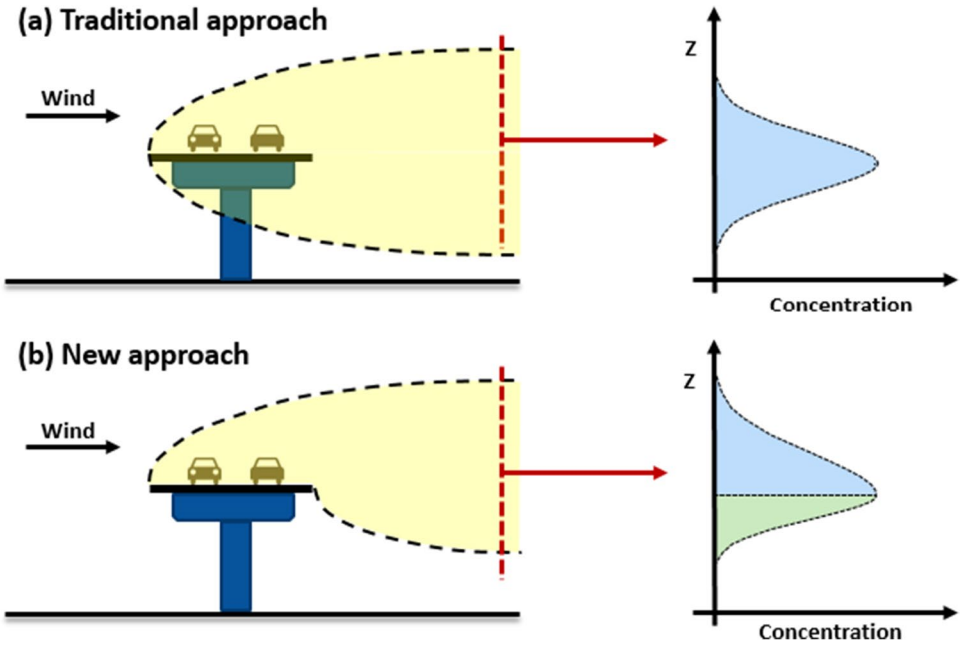

Fig. 1 Schematic illustrations of the traditional (**a**) and new (**b**) approaches to modelling elevated roads in ADMS

With the new approach (Fig. 1(b)), the vertical concentration distribution is instead described using two adjoining half-Gaussian functions that meet at the plume centreline height:

$$f(z) = a\left\{ exp\left(\frac{-\left(z-z_p\right)^2}{2\sigma_{z-}^2}\right)\left(1-H\left(z-z_p\right)\right) + exp\left(\frac{-\left(z-z_p\right)^2}{2\sigma_{z+}^2}\right)H\left(z-z_p\right) + exp\left(\frac{-\left(z+z_p\right)^2}{2\sigma_{z-}^2}\right)\right\}. \quad (3)$$

Here, H is the Heaviside step function, and σ_{z-} and σ_{z+} are the vertical spreads associated with the lower and upper parts of the plume, respectively. Note that the ground-level reflection term does not require a Heaviside step function since every point within the boundary layer is affected by this term. a is the (shared) magnitude of each half-Gaussian and follows from the constraint that the full integral of $f(z)$ must be unity. $f(z)$ can be 'unfolded' to remove the reflection term, which simplifies the integral:

$$a\left(\int_{z=-\infty}^{z=z_p} exp\left(\frac{-\left(z-z_p\right)^2}{2\sigma_{z-}^2}\right)dz + \int_{z=z_p}^{z=\infty} exp\left(\frac{-\left(z-z_p\right)^2}{2\sigma_{z+}^2}\right)dz\right) = 1 \quad (4)$$

$$\Rightarrow a = \frac{2}{\sqrt{2\pi}\left(\sigma_{z-}+\sigma_{z+}\right)} \quad (5)$$

This approach allows us to reduce the amount of material that disperses through the road surface by limiting the downward plume spread, σ_{z-}, to h_0 until the plume has passed the downwind edge of the road, after which it grows as normal. Conversely, the upward plume spread, σ_{z+}, grows unimpeded from the source. Internally, ADMS first calculates the traditional plume spread $\sigma_z(x)$ as a function of downwind distance x from the element and assigns this to $\sigma_{z+}(x)$. Then, $\sigma_{z-}(x)$ is taken to be h_0 at downwind output points inside the road segment and $\sigma_z\left(x_e\right)$ at downwind output points outside it, where x_e is the projected downwind distance from the output point to the point at which the line between the element centre and the output point intersects the road segment edge. Note that σ_z is not modified to account for any extra turbulence generated from the flyover structure itself.

Note that in calm conditions, the validity of the Gaussian-type plume approach breaks down. In ADMS-Urban / ADMS-Roads, any hours in which the input 10 m wind speed is less than 0.75 ms^{-1} will be modelled with a 10 m wind speed of 0.75 ms^{-1}, and the wind direction from the most recent hour with a 10 m wind speed greater than 0.75 ms^{-1} will be used.

Evaluation approach

Model evaluation is presented using data from two separate real-world sites where concentration measurements have been recorded close to elevated road sections. The first site is in London, UK, and the second site is in Antwerp, Belgium.

London site

This site focusses on part of the M4 flyover in Brentford, West London. Two separate automatic air quality monitoring stations are located next to this elevated stretch of motorway (Fig. 2). Both stations provide high temporal resolution (hourly) reference-quality concentration data for a range of key pollutants including NO_X and NO_2. The first station (HS010) is located next to a section of the M4 flyover that passes through Boston Manor Park, which forms the only heavily trafficked road in the immediate vicinity. The second station (HS5) is located next to a section of the M4 flyover that runs above another busy road, the A4. The HS010 monitor is approximately 7 m from the edge of the M4 and has an inlet height of 1.7 m. The HS5 monitor is approximately 9 m from the edge of the M4 (4.5 m from the edge of the A4) with an estimated inlet height of 2.5 m. The M4 road surface is approximately 6 m above ground level near both monitors. One full year (2019) of monitoring data was used to validate the ADMS model.

In ADMS, a 3 km stretch of the M4 flyover and the ground-level A4 close to the monitors were modelled as explicit road sources. For the M4, hourly traffic flow data was available from Highways England's WebTRIS dataset (Highways England 2021). This was used to generate the traffic flow data required by the model (vehicle category, average speed, annual-average number of vehicles per hour) along with an hourly time-varying emission factors file. For the A4, only a single 12-h monitoring period of vehicle count data from the Department for Transport (DfT) was available. The WebTRIS M4 data was used to scale these vehicle counts to other periods in order to calculate the annual-average number of vehicles per hour, and to generate diurnal time-varying emission factor profiles split by weekdays, Saturdays and Sundays. NO_X emission factors were taken from Defra's Emission Factors Toolkit (EFT) version 9 (Defra 2019) but were adjusted up by approximately 40% following the methodology set out in Hood et al. (2018) that attempts to correct for the apparent discrepancy between published emission factors and 'real-world' emissions for older vehicle types.

Volume sources of variable horizontal dimension but fixed depth (10 m) were used to model emissions from all other sources in a 26×26 km region surrounding the study site, with the smallest (1×1 km) sources used over the study site. (Total) emission rates were taken from the National Atmospheric Emissions Inventory (NAEI; Tsagatakis et al. 2021)—the explicit road source emissions are disaggregated from these totals by the model at run-time to avoid double counting. Background concentration data representing longer range pollutants advected into the modelling region were taken from one of four 'rural background' reference monitoring sites (Lullington Heath, Chilbolton, Rochester Stoke, and Wicken Fen) depending on the wind direction for each hour. The hourly meteorological data was taken from the Met Office's automatic weather station at the nearby Heathrow Airport. Fast local NO_X chemistry was modelled using the ADMS Chemical Reaction Scheme (Smith et al. 2017). Finally, the section of the A4 next to the HS5 monitor was modelled as a single-sided street canyon using the advanced street canyon module within ADMS (Hood et al. 2021) in order to account for the row of tall buildings adjacent to the monitor (Fig. 2). The elevated M4 was not modelled using the street canyon parameterisation.

Antwerp site

The Antwerp dataset was collected during a monitoring campaign that is described in detail in Van Poppel et al. (2012), though a summary is also given here. Two air quality

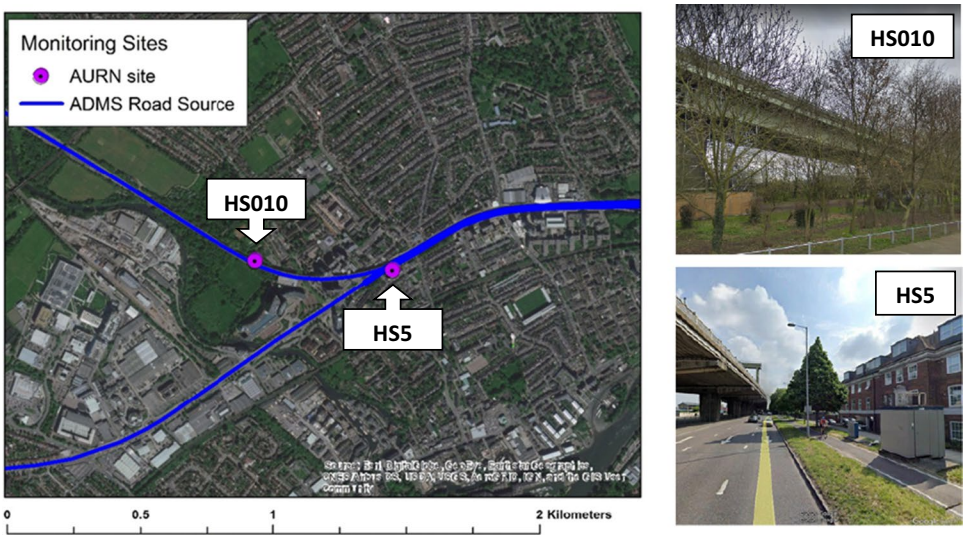

Fig. 2 Left: Map of London site showing the location of both air quality monitors and the explicitly modelled road sources in ADMS, Source: ESRI et al. Right: Google Street View® images in the immediate vicinity of each air quality monitor

monitors were positioned either side of a ground-level section of the busy R1 ring road and later moved to a nearby elevated section of the same road in order to compare the difference that road elevation makes to near-ground-level concentrations (Fig. 3). The monitor locations next to the ground-level section were 29 m and 102 m away from the nearest road edge, and the monitor locations next to the elevated section were 60 m and 120 m from the nearest road edge. The inlet height was 2 m in all cases. The campaign lasted a total of 3 months (February–April 2009) with data collected every minute and then averaged over 30-min periods. Meteorological data was also available from a nearby weather station with 30-min time resolution. The wind direction was used to define which monitor was the 'upwind' monitor and which was the 'downwind' monitor when calculating the road increment. Wind directions that were within 30° of being parallel with the relevant road section were discounted from the analysis.

In ADMS, the ground-level and elevated (12 m) sections of the motorway close to the monitors were explicitly modelled as (separate) road sources. Because measured concentrations were available on either side of the road, and only periods for which there was a clear upwind/downwind monitor were considered, there was no need to model any other sources or define any background data—the output concentrations could be compared directly with the measured road increment (there were no other major roads between the monitor and the motorway in all cases). Traffic emissions were calculated using estimates from Van Poppel et al. (2012) of 200,000 vehicles per day on the ground-level road section with a light/heavy-duty vehicle split of 0.776:0.224, and 23.2% fewer vehicles per day on the elevated road section (due to the presence of a slip road between the two road sections) with a light/heavy-duty vehicle split of 0.739:0.261. A representative set of diurnal time-varying emission factors (for weekdays, Saturdays and Sundays) was used. An average vehicle speed of 80 km/h was assumed for both vehicle categories. Resulting emissions were calculated using EFT version 6, the latest version to include emission factors for the monitoring campaign year (2009). No adjustments were made to these emission factors, which are higher than those in later EFT releases (Marner 2016). The road increment evaluation approach is only applicable to conserved pollutants, so only total NO_X concentrations at this site are analysed and the ADMS model local chemistry scheme was not required. Since the model expects hourly input data but measurements were provided half-hourly, four runs were performed: ground-level road section monitoring period on the hour, ground-level road section monitoring period on the half-hour, elevated road section monitoring period on the hour, elevated road section monitoring period on the half-hour.

The "Sensitivity analysis" section below also presents a model sensitivity analysis looking at the ratio of concentrations from an elevated road source with those from an equivalent ground-level road source. In order to utilise the data from the Antwerp monitoring campaign for validation, it was first necessary to post-process the raw data to strive towards a like-for-like comparison between the concentrations recorded near the ground-level and elevated road sections. The main factors preventing a direct comparison between the raw data from the two road sections

Fig. 3 Map of Antwerp site showing all four monitoring locations and the explicitly modelled road sources in ADMS, ©Openstreet Map. Inset: Google Street View® image near 'Elevated B' monitor location

are summarised below, along with a description of how each factor has been accounted for in the post-processing of the raw data:

- **Different background concentrations** – Data from the two road sections were collected during different monitoring periods, which will have been affected by long-range pollutant transport to differing extents. This was accounted for by always using the road concentration increment, i.e. subtracting the NO_X concentration recorded at the upwind monitor from the value recorded at the downwind monitor (no other major roads lie between the monitor and the motorway in all cases).
- **Different traffic flows** – Concentrations are proportional to the source emission term, and traffic flows are different on the two road sections due to the presence of a slip road between them. Concentrations were therefore normalised by the traffic flow rate to give 'concentration per vehicle' values.
- **Different source-to-receptor distances** – Concentrations are affected by the distance from the source term, particularly closer to the source where gradients are high. NO_X concentration decay factors were applied to the normalised road increments from the ground-level road section to simulate moving the relevant monitor from its original location (102 m or 29 m from the nearest road edge) to the equivalent location of the elevated road section monitor (120 m or 60 m from the nearest road edge). The decay factors were calculated from an ADMS model configuration for the ground-level road section in which additional receptor points at the elevated road section monitor distances were included.
- **Different atmospheric conditions** – Meteorological conditions affect dispersion, and different periods have different distributions of meteorological conditions. Wind speed is a particularly influential variable on near-field dispersion characteristics, both directly and indirectly through associations with different atmospheric stability classes (Pasquill 1961). The normalised distance-adjusted road increments were therefore binned into one of five wind speed classes (<2, 2–4, 4–6, 6–8, and >8 m s^{-1}) and the weighted average calculated. This was done for each road section (ground-level and elevated) for each road-receptor distance (120 m and 60 m), leading to four data points from which two elevated-to-ground-level concentration ratios were calculated.

Other factors, such as differences in surface characteristics in the vicinity of the ground-level and elevated road sections, have not been accounted for.

Results and discussion

Model validation

We start by comparing modelled versus monitored period-average concentrations (or concentration increments) for each of the monitors located next to an elevated road section (concentrations for HS010 and HS5 at the London site, and concentration increments for 'Elevated A' and 'Elevated B' at the Antwerp site). These results are presented in Fig. 4. Modelled results are shown for two separate model configurations; one in which the elevated road sections are modelled at ground level ('Flat') and another in which they are modelled at the correct height using the new elevated roads approach ('New'). For the HS010 receptor, results from a third model configuration are also presented in which the elevated road section is modelled at the correct height but using the traditional elevated roads approach ('Old'). This was the only receptor where the adjacent elevated road was largely isolated from any other roads and detailed hourly traffic flow data were available; we can therefore have higher confidence when comparing the 'Old' and 'New' configuration results. For the other receptors, the magnitude of the uncertainty in the source emission term is potentially

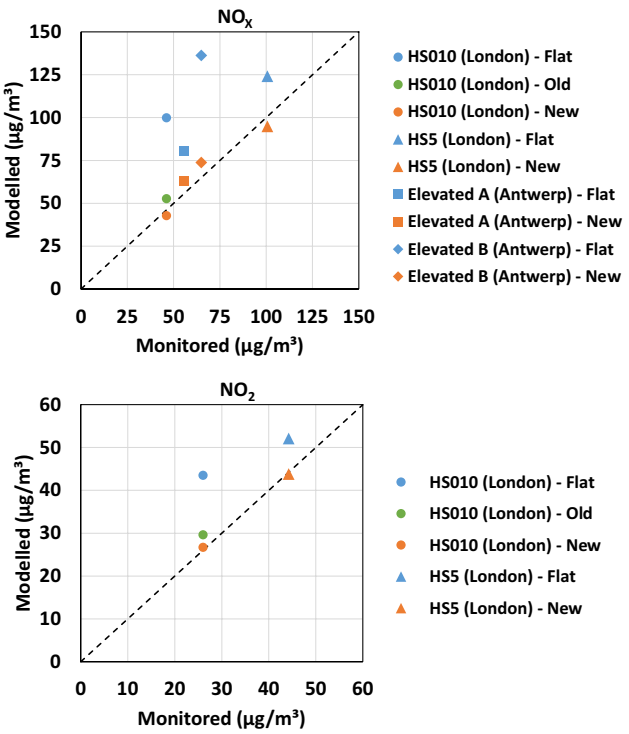

Fig. 4 Modelled versus monitored period-average concentrations (HS010, HS5) or concentration increments (Elevated A, Elevated B) for each monitor located next to an elevated road section for pollutants NO_X (top) and NO_2 (bottom)

comparable with the differences between the 'Old' and 'New' configuration results, particularly in Antwerp where a fairly crude estimate of the total traffic flow has been used.

There is a significant improvement in the modelled period-average concentrations at all receptors when the elevated road is modelled at the correct height rather than at ground level. Modelling the elevated road at ground level leads to large over-predictions, sometimes by as much as double the measured concentration. The new modelling approach predicts these period-average concentrations very well, with little overall bias (some data points fall slightly above the $x = y$ line, others slightly below). The old modelling approach leads to a slight over-prediction at the HS010 receptor for both NO_X and NO_2, which is likely due to its failure to account for the shielding effect of the road surface on the downward spread of the plume towards the receptor. However, accounting for road elevation in general has a much more significant bearing on model accuracy than the choice of elevated road modelling approach in this case; modelling the road at ground level leads to an over-prediction of 116% for NO_X (67% for NO_2), while modelling the road at elevation leads to an over-prediction of 14% for NO_X and NO_2 using the old approach compared with an under-prediction of 7% for NO_X (over-prediction of 3% for NO_2) using the new approach.

It is informative to review other model performance statistics calculated from the hourly concentration values. Table 1 shows, for each monitor-pollutant-modelling approach combination, the normalised mean square error (NMSE), correlation coefficient (r), fraction of modelled concentrations within a factor of two of the monitored values (fac2), and fractional bias (fb). NMSE and fb have an ideal value of zero while r and fac2 have an ideal value of one. These additional metrics confirm that modelling the road at elevation is important to achieve adequate modelling accuracy at all monitor locations. Fractional bias is particularly reduced; there are no values with a magnitude greater than 0.08 at the London site using the new modelling approach, compared with fractional biases of up to 0.74 when modelling the elevated road at ground level. The fractional bias at the two Antwerp site receptors (where traffic flow estimates are less reliable) is both 0.13 with the new modelling approach compared with 0.37 and 0.71 when modelling the elevated road at ground level. Comparing the old and new modelling approaches at the HS010 monitor, the new approach leads to improved results for all but one statistic (NMSE for NO_X).

Source apportionment

Next, we use the new approach to look at source apportionment for the cases where multiple sources were modelled (London site). Figure 5 shows modelled annual-average NO_X source apportionment results at each London receptor, where the data have been binned into 10° wind sectors. The individual contributions from the explicitly modelled elevated (M4) and ground-level (A4) road sources, other local sources (modelled as volume sources), and the background concentration representing longer range pollutant transport into the modelling region are presented. Also shown are the corresponding annual-average monitored concentrations (black dots) and their standard deviations (whiskers) for each wind sector. The sample sizes for each wind sector range between 88 and 511 at the HS010 monitor and 93 and 529 at the HS5 monitor. There is generally good agreement in terms of the magnitude of total modelled concentrations across the different wind sectors, providing further confidence in the new modelling approach.

At both receptors, there is a clear variation of elevated road source contribution with wind direction. The bearing of the M4 from north is approximately 120°/300° near the HS010 receptor and 70°/250° near the HS5 receptor. Higher concentrations are apparent when the wind is blowing parallel with the road. The contribution falls to zero when the wind is perpendicular to the M4 such that emissions are advected away from the monitor side of the road, as would be expected. For the opposite perpendicular wind direction (emissions advected towards the monitor side of the road), the M4 contribution also reduces to close to zero at the HS010 receptor, indicating the plume passes over the

Table 1 Modelled statistics. Best statistics (per monitor-pollutant pair) are shaded grey

Monitor	Pollutant	Approach	# valid data points	Monitored mean (µg/m³)	Modelled mean (µg/m³)	NMSE	r	fac2	fb
HS010	NO_X	Flat	8666	46.2	99.8	2.44	0.34	0.36	0.76
HS010	NO_X	Old	8666	46.2	52.6	1.21	0.52	0.62	0.13
HS010	NO_X	New	8666	46.2	42.8	1.29	0.56	0.71	-0.08
HS010	NO_2	Flat	8666	26.0	43.5	0.87	0.50	0.58	0.50
HS010	NO_2	Old	8666	26.0	29.6	0.39	0.63	0.79	0.13
HS010	NO_2	New	8666	26.0	26.7	0.36	0.65	0.80	0.03
HS5	NO_X	Flat	8666	100.7	124.1	0.62	0.66	0.80	0.21
HS5	NO_X	New	8666	100.7	94.9	0.43	0.69	0.87	-0.06
HS5	NO_2	Flat	8666	44.3	52.1	0.31	0.68	0.87	0.16
HS5	NO_2	New	8666	44.3	43.8	0.19	0.71	0.90	-0.01
Elevated A	NO_X	Flat	476	55.5	80.5	0.33	0.82	0.76	0.37
Elevated A	NO_X	New	476	55.5	63.1	0.15	0.88	0.91	0.13
Elevated B	NO_X	Flat	359	65.0	136.2	0.97	0.71	0.46	0.71
Elevated B	NO_X	New	359	65.0	73.8	0.17	0.90	0.91	0.13

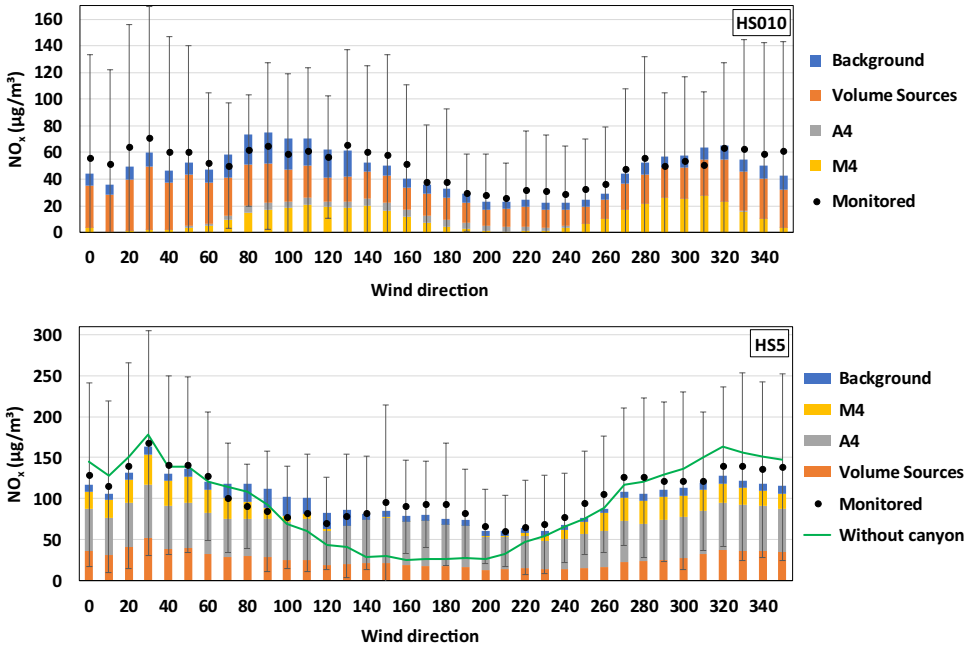

Fig. 5 Modelled source apportionment results, using the new elevated road approach, for annual-average NO_X for each 10° wind sector at the HS010 site (top) and HS5 site (bottom). Black dots and whiskers show corresponding annual-average monitored concentrations and their standard deviations. Green line in bottom panel shows total modelled concentrations when the A4 is modelled as an open road source rather than as an asymmetric canyon

monitor before it has a chance to disperse down to the height of the monitor. The relatively reduced impact arising from perpendicular winds is also apparent at the HS5 receptor but is less pronounced since the receptor is higher and further from the edge of the M4, and the curvature of the M4 is more pronounced at this location. When the wind blows parallel to the elevated road, the plume has a longer time to disperse downwards after leaving the road surface before reaching the monitor, hence the larger contribution for parallel wind directions.

At the HS5 receptor, where both the elevated M4 and the ground-level A4 roads run close to the monitor, the receptor concentrations are seen to be significantly more affected by the A4 than the M4. This is despite the fact that the A4 emissions are approximately half of those from the M4, although it must be noted that the A4 is horizontally closer to the receptor than the M4. This highlights the mitigating effect that road elevation can have on near-ground concentration levels. The comparatively low impact of the elevated road is explained not only by the increased vertical distance between the source and the receptor but also by the fact that the wind speed increases with height, which typically leads to greater dispersion (faster dilution) of the plume with downwind distance. Furthermore, ground-level sources experience reflections immediately, up-to doubling the ground-level concentrations, whereas for elevated sources, these reflections are delayed and do not occur along the plume centreline, leading to relatively lower concentrations at a given downwind distance.

Unlike the elevated M4, the ground-level A4 contribution at the HS5 receptor is fairly consistent across all wind directions. For a road in open surroundings, we would expect the contribution to reduce when the wind blows emissions away from the monitor side of the road. However, the row of buildings adjacent to the HS5 monitor creates an asymmetric street canyon, which leads to the formation of a recirculating cell that acts to recycle the road emissions back towards the monitor. The green line in Fig. 5 (bottom panel) shows total modelled concentrations when the A4 is modelled as an open road source rather than as an asymmetric canyon. In this configuration, concentrations are much lower when the wind blows from the receptor towards the road sources, as expected, but this leads to significant under-predictions compared with the total monitored concentrations. This highlights the importance of accounting for street canyon effects in urban dispersion modelling. It also highlights another advantage of road elevation with respect to mitigating near-ground concentrations; if the road is elevated above the height of any adjacent rows of buildings, the effects of pollutant trapping due to street canyon recirculation are largely avoided. If the elevated road still lies within the street canyon, canyon recirculation effects should still be considered.

Air quality maps

The above metrics provide confidence in the ability of the new modelling approach to predict measured concentrations close to elevated roads. For example, the fractional bias is limited to 0.15, the fraction of modelled values within a factor of two of monitored is at least 0.7, and the correlation ranges from 0.56 to 0.9 across all cases presented. We therefore progress to using the new model to generate air quality maps of the local area. Figure 6 shows contour plots of

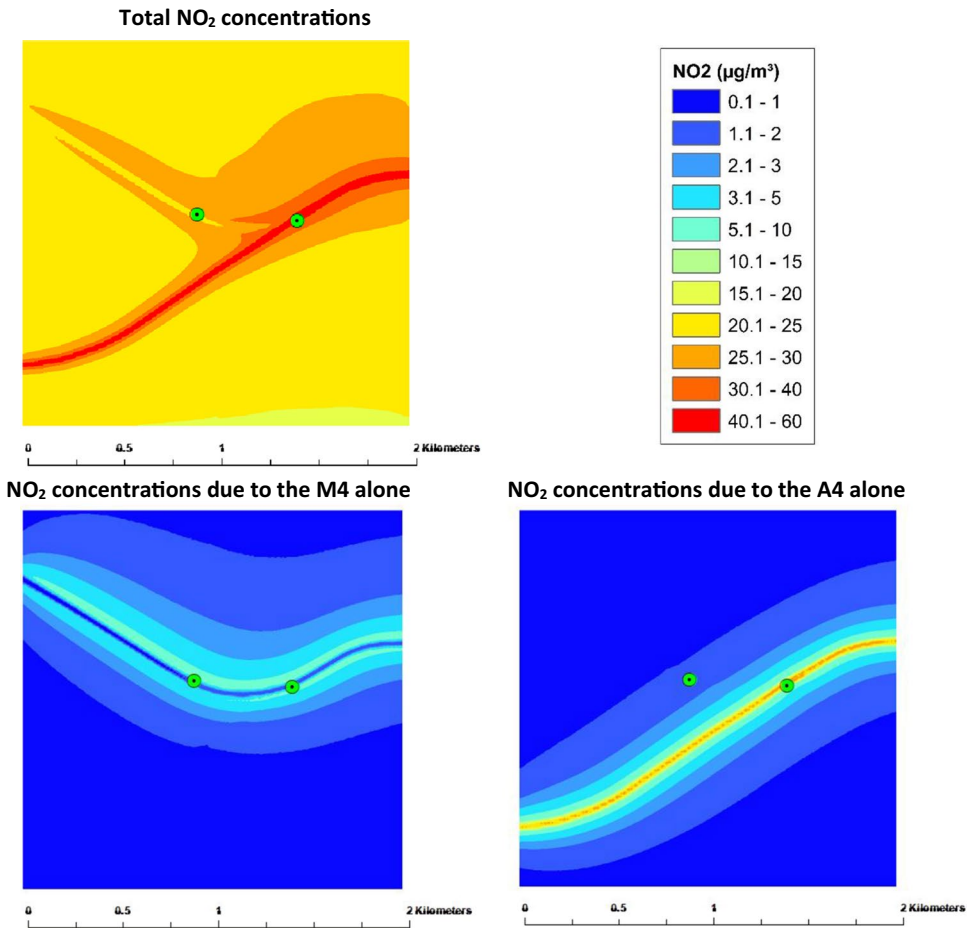

Fig. 6 Annual-average contour plots of modelled NO_2 concentrations at 1.5 m above ground level at the London site. Total concentrations are shown (top left) as well as indicative contributions from the elevated M4 (bottom left) and ground-level A4 (bottom right) alone. Green dots show monitor locations

modelled annual-average NO_2 concentrations in the vicinity of the two London monitors. The output grid is at a height of 1.5 m. Total concentrations are shown, as well as the individual contributions from the elevated M4 and ground-level A4 road sources. Note, however, that the single source calculations are 'indicative' as it is not possible to perform direct source apportionment for NO_2 due to the non-linearity of NO_X chemistry.

The influence of road elevation on reducing the near-ground concentrations is evident, with a much stronger signature from the A4 than from the M4. The impact of the ground-level road is strongest along the road centreline, reducing in both directions with increasing distance from the road. Conversely, there is a clear concentration 'shadow' directly underneath the elevated road, with the maximum concentrations occurring as two parallel peaks either side of the road centreline.

Sensitivity analysis

Finally, we present the results of a sensitivity analysis in which the new approach was used to model an isolated elevated road at various heights. These results can aid modellers in deciding when it is necessary to model an elevated road at its true elevation rather than at ground level, which will mainly depend on the height of the road as well as the distance from the road to the receptor(s) of interest. Urban planners can also use these results to gauge the relative benefit of road height on maximum near-ground concentrations when designing new flyovers.

The same road width, road orientation, traffic emissions, and meteorological data that were used for modelling the London M4 flyover near the HS010 monitor were employed. This setup can be considered broadly representative of a typical elevated motorway site, in the UK at least, though it is acknowledged that differences in these model inputs would lead to slightly different results. The results presented here should therefore only be used as a guide and it is advised to repeat similar sensitivity analyses in which the source setup and meteorological data are appropriate to the particular study site being considered. A single row of receptor points was placed perpendicular to the road centreline, at a height of 2 m to allow comparison with the Antwerp monitoring campaign dataset.

Figure 7 shows period-average modelled NO_X concentration profiles as a function of distance from the road

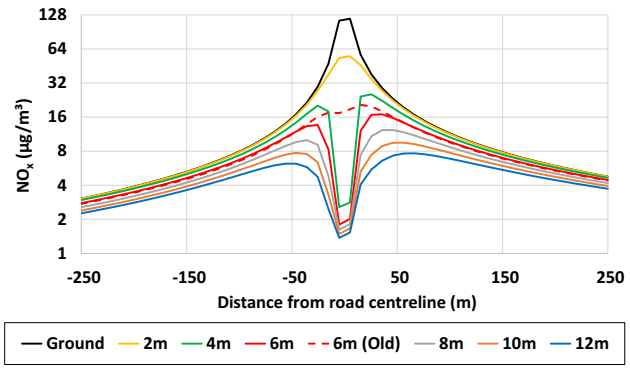

Fig. 7 Period-average modelled NOx concentrations (at 2 m) as a function of distance from the road centreline for various road elevations. Model setup is the same as that used for the M4 flyover next to the HS010 monitor but only the motorway increment is considered. New elevated road modelling approach used in all cases except the dashed line profile, which uses the old approach

centreline for road elevations of 0 (ground-level), 2, 4, 6, 8, 10, and 12 m. It can be seen that the ground-level road source leads to significantly higher maximum concentrations, which quickly fall away as the road elevation increases (note the use of the logarithmic scale on the *y*-axis). For example, the maximum 2 m concentration reduces from 118 µg m^{-3} for a ground-level road source to just 16.9 µg m^{-3} for a road source at 6 m (a reduction of 85.6%). As was seen in the contour plots above, the maximum concentrations occur in line with the road centreline for the ground level and 2 m road sources, both of which are below or at the height of the receptors, whereas a local minimum is observed under the centreline of the other road sources, which are elevated above the receptors. For the higher road elevations, two local maxima occur either side of the road centreline. The distances at which these maxima occur increase as the road elevation increases, which is not surprising as the plume has to travel further before it reaches the ground. For example, for positive receptor distances, the 2 m maximum concentration occurs at around 20 m from the road centreline for a 4 m road source and at around 70 m from the road centreline for a 12 m road source. There is a clear signature of the prevailing wind (south-westerly in the UK) in these results, with higher period-average concentrations to the north-east of the road (positive receptor distances). It should be noted that while the concentration profiles presented in the figure show the elevated road concentrations as lower than the corresponding ground-level road values in the near field, in the far field (not shown), the elevated road profiles decay to a slightly higher value; for example, the concentration associated with the 2 m road source exceeds that from the ground-level road source at around 285 m. Thus, increasing the road elevation reduces the peak near-ground concentration significantly but also impacts a wider area (corroborating Joerger and Pryor 2018). While the concentrations from individual road sources are comparatively low at these large distances, the cumulative effect may be significant across large urbanisations.

Also shown in Fig. 7 by the dashed line is the profile for the 6 m road source (same height as the M4 flyover) using the old elevated road modelling approach in which the shielding effect of the road surface is not accounted for. It can be seen that the modelled 2 m concentrations differ significantly from those obtained using the new modelling approach (which does account for road surface shielding) at receptors that are up to around 40 m from the road centreline. After this point, the choice of elevated road modelling approach does not significantly affect modelled concentrations. Conversely, the need to account for road elevation in general remains important at much greater distances from the road. This is better demonstrated in the next figure.

Figure 8 shows the same data as that used in Fig. 7 but expressed as the ratio of the elevated road concentration to the ground-level road concentration. The ratios derived from the Antwerp field campaign dataset (as described in the "Antwerp site" section) are overlaid on these profiles (black circles). The Antwerp motorway has a height of 12 m. Despite the different road source geometry and meteorological conditions, the Antwerp measured ratios compare very well with the modelled 12 m profile, providing further confidence in the ability of the model to accurately predict concentrations in the vicinity of elevated roads. The profiles show that the impact of road elevation initially decreases rapidly with distance from the road in all cases, but asymptotes much more slowly as the road elevation increases. For example, by 250 m from the road centreline, the concentration from a road source with an elevation of 4 m is within 3% of the concentration from an equivalent ground-level road source, whereas the concentration from a 12 m road source

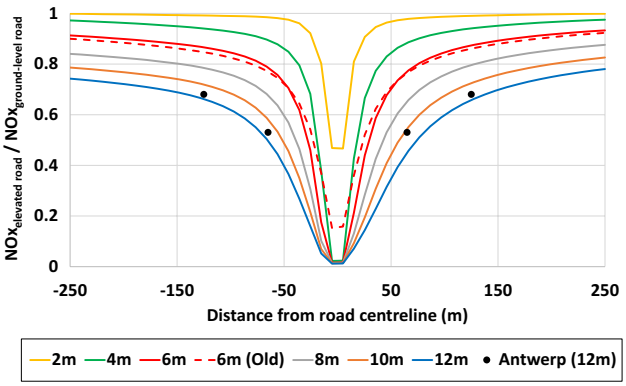

Fig. 8 As in Fig. 7 but expressed as the ratio of the elevated road concentration to the ground-level road concentration. Dots show processed measurement data from the Antwerp field campaign, where the motorway was 12 m above ground

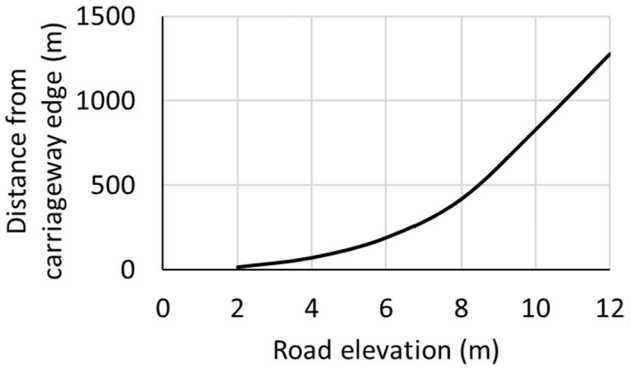

Fig. 9 Typical distance from an elevated road at which the 2 m concentration contribution reduces to within 10% of the 2 m concentration contribution from an equivalent ground-level road

is still around 25% lower than the concentration from an equivalent ground-level road source. Figure 9 shows the distance from the road centreline at which the 2 m concentration contribution from each of these road elevations reduces to within 10% of the 2 m concentration contribution from the equivalent ground-level road source. These results show that it is necessary to travel well over 1 km from a 12 m high road source for the effects of modelling road elevation on the near-ground concentrations to become largely insignificant (< 10%).

Conclusions

This study has demonstrated the importance of accounting for road elevation when performing local air quality modelling for predicting near-road concentrations. Road elevation can significantly reduce ground-level pollutant concentrations as a result of (i) increased source-receptor distance, (ii) increased dilution from the source due to higher wind speeds, (iii) reduced effect of ground-level plume reflections, and (iv) reduced effect of pollutant recirculation/trapping in cases where the road is elevated above a street canyon.

A new approach to modelling elevated roads has also been implemented in the operational quasi-Gaussian dispersion model ADMS. With this approach, rather than simply raising the height of the road source and allowing the plume to disperse freely through the road surface, the downward plume spread is limited until the plume has cleared the road carriageway to account for the effect of road surface shielding. The new model was evaluated against measurements from two reference monitors next to an elevated motorway section in London, UK, and against measurements taken during a monitoring campaign near an elevated section of ring road in Antwerp, Belgium (Van Poppel et al. 2012). Model performance was good at all receptors, with period-average concentrations within − 7.4% to + 14% of monitored values, compared with over-predictions as large as 116% when the elevated road sections were modelled at ground level. The new modelling approach was also shown to perform slightly better than the traditional approach, which tended to slightly over-predict near-ground concentrations as a result of allowing material to disperse freely down through the road surface.

A source apportionment analysis by wind direction at the London site indicates that maximum near-ground concentrations occur when the wind blows parallel with the road as the plume has more time to disperse down to the level of the monitor before passing over it. Furthermore, a sensitivity analysis was presented in which multiple road elevations were modelled and near-ground concentrations compared against those from an equivalent ground-level road source. These results can be used by dispersion modellers for determining whether it is important to account for road elevation, or by urban planners when designing new flyovers.

An interesting continuation of this work would be to consider improvements to the way in which embankments are modelled. Unlike flyovers, air cannot flow underneath an embanked road and so streamline convergence and divergence will occur, affecting the dispersion of traffic emissions. This study has focussed on near-ground-level concentrations and thus largely concerns outdoor pollutant exposure, but it would also be interesting to analyse the effects of flyovers on the vertical concentration distribution, which is important in the context of indoor air quality within multi-storey buildings. Another extension of this work would be to consider the joint effects of elevated roads and street canyons in cases where the flyover is below the local building level. Finally, the conclusions in this study would also be strengthened with further model validation, which would rely on the availability of datasets from field campaigns and/or wind-tunnel/CFD studies of dispersion from flyovers.

Acknowledgements We are grateful to Highways England for their input during the project.

Funding This study was funded by Highways England under the Small Business Research Initiative (SBRI) Innovate UK competition 'Developing digital roads and improving air quality'.

Data availability The datasets associated with the London site evaluation are available from the corresponding author on reasonable request. The datasets associated with the Antwerp site evaluation may be available from Martine Van Poppel (VITO) but restrictions apply.

Declarations

Ethics approval and consent to participate Not applicable.

Consent for publication Not applicable.

Competing interests The authors declare no competing interests.

References

Baldwin N, Gilani O, Raja S, Batterman S, Ganguly R, Hopke P, Berrocal V, Robins T, Hoogterp S (2015) Factors affecting pollutant concentrations in the near-road environment. Atmos Environ 115:223–235. https://doi.org/10.1016/j.atmosenv.2015.05.024

Beckerman B, Jerrett M, Brook JR, Verma DK, Arian MM, Finkelstein MM (2008) Correlation of nitrogen dioxide with other traffic pollutants near a major expressway. Atmos Environ 42:275–290. https://doi.org/10.1016/j.atmosenv.2007.09.042

Cai M, Huang Y, Wang Z (2020) Dynamic three-dimensional distribution of traffic pollutant at urban viaduct with the governance strategy. Atmos Pollut Res 11:1418–1428. https://doi.org/10.1016/j.apr.2020.05.002

Carruthers DJ, Edmunds HA, Lester AE, McHugh CA, Singles RJ (2000) Use and validation of ADMS-Urban in contrasting urban and industrial locations. Int J Environ Pollut 14:364–374. https://doi.org/10.1504/IJEP.2000.000558

Caton F, Britter RE, Dalziel S (2003) Dispersion mechanisms in a street canyon. Atmos Environ 137:693–702. https://doi.org/10.1016/S1352-2310(02)00830-0

CERC (2021) ADMS Technical Specifications, available online at http://www.cerc.co.uk/TechSpec (accessed December 2021)

Cimorelli AJ, Perry SG, Venkatram A, Weil JC, Paine RJ, Wilson RB, Lee RF, Peters WD, Brode RW (2005) AERMOD: a dispersion model for industrial source applications. Part I: General Model Formulation and Boundary Layer Characterization. J Appl Meteorol Climatol 44:682–693. https://doi.org/10.1175/JAM2227.1

Defra (2019) Emissions Factors Toolkit v 9.0 User Guide, available at https://laqm.defra.gov.uk/documents/EFTv9-user-guide-v1.0.pdf (accessed December 2021)

Defra (2021) Automatic Urban and Rural Network (AURN), available at: https://uk-air.defra.gov.uk/networks/network-info?view=aurn (accessed December 2021)

Fenger J (1999) Urban air quality. Atmos Environ 33:4877–4900. https://doi.org/10.1016/S1352-2310(99)00290-3

Hang J, Luo Z, Wang X, He L, Wang B, Zhu W (2017) The influence of street layouts and viaduct settings on daily carbon monoxide exposure and intake fraction in idealized urban canyons. Environ Pollut 220:72–86. https://doi.org/10.1016/j.envpol.2016.09.024

Heist DK, Perry SG, Brixley LA (2009) A wind tunnel study of the effect of roadway configurations on the dispersion of traffic-related pollution. Atmos Environ 43:5101–5111. https://doi.org/10.1016/j.atmosenv.2009.06.034

Highways England (2021) WebTRIS, available at https://webtris.highwaysengland.co.uk (accessed December 2021)

Hitchins J, Morawska L, Wolff R, Gilbert D (2000) Concentrations of submicrometre particles from vehicle emissions near a major road. Atmos Environ 34:51–59. https://doi.org/10.1016/S1352-2310(99)00304-0

Hood C, MacKenzie I, Stocker J, Johnson K, Carruthers D, Vieno M, Doherty R (2018) Air quality simulations for London using a coupled regional-to-local modelling system. Atmos Chem Phys 18:11221–11245. https://doi.org/10.5194/acp-18-11221-2018

Hood C, Stocker J, Seaton M, Johnson K, O'Neill J, Thorne L, Carruthers D (2021) Comprehensive evaluation of an advanced street canyon air pollution model. J Air Waste Manag Assoc 71:247–262. https://doi.org/10.1080/10962247.2020.1803158

Joerger VM, Pryor SC (2018) Ultrafine particle number concentrations and size distributions around an elevated highway viaduct. Atmos Pollut Res 9:714–722. https://doi.org/10.1016/j.apr.2018.01.008

Kampa M, Castanas E (2008) Human health effects of air pollution. Environ Pollut 151:362–367. https://doi.org/10.1016/j.envpol.2007.06.012

Kumar A, Patil RS, Dikshit AK, Islam S, Kumar R (2015) Evaluation of control strategies for industrial air pollution sources using American Meteorological Society/Environmental Protection Agency Regulatory Model with simulated meteorology by Weather Research and Forecasting Model. J Clean Prod 116:110–117. https://doi.org/10.1016/j.jclepro.2015.12.079

Lu K-F, He H-D, Wang H-W, Li X-B, Peng Z-R (2020) Characterizing temporal and vertical distribution patterns of traffic-emitted pollutants near an elevated expressway in urban residential areas. Build Environ 172:106678. https://doi.org/10.1016/j.buildenv.2020.106678

Marner B (2016) Overview of changes introduced by EFT v7.0 and by CURED v2a. *Air Quality Consultants*, available online at https://www.aqconsultants.co.uk/CMSPages/GetFile.aspx?guid=dfba9f91-0351-4f8f-ab25-9d26f94bc8b3 (accessed December 2021)

Oke TR (1988) Street design and urban canopy layer climate. Energy Build 11:103–113. https://doi.org/10.1016/0378-7788(88)90026-6

Pasquill F (1961) The estimation of the dispersion of windborne material. Meteorol Mag 90:33–49

Sala A (2013) Assessment of traffic flow benefits of flyovers: a case study. J Traffic Transp Eng 4:1–9

Smith S, Stocker J, Seaton M, Carruthers D (2017) Model inter-comparison and validation of ADMS plume chemistry schemes. Int J Environ Pollut 62:395–406. https://doi.org/10.1504/IJEP.2017.089427

Snyder MG, Venkatram A, Heist DK, Perry SG, Petersen WB, Isakov V (2013) RLINE: A line source dispersion model for near-surface releases. Atmos Environ 77:748–756. https://doi.org/10.1016/j.atmosenv.2013.05.074

Tominaga Y, Stathopoulos T (2013) CFD simulation of near-field pollutant dispersion in the urban environment: a review of current modelling techniques. Atmos Environ 79:716–730. https://doi.org/10.1016/j.atmosenv.2013.07.028

Tsagatakis I, Richardson J, Evangelides C, Pizzolato M, Pearson B, Passant N, Pommier M, Otto A (2021) UK Spatial Emissions Methodology: a report of the National Atmospheric Emission Inventory 2019. Retrieved from: https://naei.beis.gov.uk/reports/reports?report_id=1024

Van Poppel M, Panis LI, Govarts E, Van Houtte J, Maenhaut W (2012) A comparative study of traffic related air pollution next to a motorway and a motorway flyover. Atmos Environ 60:132–141. https://doi.org/10.1016/j.atmosenv.2012.06.042

Vardoulakis S, Valiantis M, Milner J, ApSimon H (2007) Operational air pollution modelling in the UK – street canyon applications and challenges. Atmos Environ 41:4622–4637. https://doi.org/10.1016/j.atmosenv.2007.03.039

World Health Organization (WHO) (2021) WHO global air quality guidelines: particulate matter (PM2.5 and PM10), ozone, nitrogen dioxide, sulfur dioxide and carbon monoxide. World Health Organization. https://apps.who.int/iris/handle/10665/345329

Wu C-L, He H-D, Song R-F, Peng Z-R (2022) Prediction of air pollutants on roadside of the elevated roads with combination of pollutants periodicity and deep learning method. Build Environ 207:108436. https://doi.org/10.1016/j.buildenv.2021.108436

Zhi H, Qiu Z, Wang W, Wang G, Hao Y, Liu Y (2020) The influence of a viaduct on PM dispersion in a typical street: field experiment and numerical simulations. Atmos Pollut Res 11:815–824. https://doi.org/10.1016/j.apr.2020.01.009